TITLE

ASSESSING CENTRAL NERVOUS SYSTEM AND PERIPHERAL NERVOUS SYSTEM FUNCTIONING IN RESTING AND NON-RESTING CONDITIONS IN A HEALTHY ADULT POPULATION: A FEASIBILITY STUDY

AUTHORS

Tyson M. Perez, DC, PhD[1*]; Emily Drake, MS[1]; Stephanie Sullivan, DC, PhD[1]

AFFILIATIONS

[1]Dr. Sid E. Williams Center for Chiropractic Research, Life University, Marietta, Georgia, USA.

*Corresponding author: Tyson M. Perez; email: tyson.perez@life.edu

FUNDING

This trial was funded by Life University's Center for Chiropractic Research.

CONFLICT OF INTEREST STATEMENT

The authors declare no competing interests.

ARTIFICIAL INTELLIGENCE (AI)

AI technology was not used in this manuscript's production.

ACKNOWLEDGEMENTS

We thank Dusty Baker and Austin Garlinghouse for their efforts with participant recruitment and data collection. We also thank Johnathon Moore, PhD, for his help with study design and methodology development.

AUTHOR CONTRIBUTIONS

All authors contributed to study design and approved the final manuscript. ED collected the data. ED and TP performed signal preprocessing and data analyses. The manuscript was drafted by TP and ED, and critically evaluated and edited by SS.

TITLE

ASSESSING CENTRAL NERVOUS SYSTEM AND PERIPHERAL NERVOUS SYSTEM FUNCTIONING IN RESTING AND NON-RESTING CONDITIONS IN A HEALTHY ADULT POPULATION: A FEASIBILITY STUDY

ABSTRACT

Emerging research suggests that chiropractic adjustments and spinal manipulative therapy (SMT) modulate the activity of the central and peripheral nervous systems (CNS and PNS); however, robust methodologies to investigate both systems in tandem are currently lacking in this space. This feasibility study sought to test a newly developed battery which incorporates robust, evidence informed methods for neurophysiological data collection across resting and non-resting conditions. We enrolled a convenience sample of 11 adults in and around Atlanta, Georgia. Signals captured during resting and non-resting states included electroencephalography (EEG), respiration, electrocardiography (ECG), impedance cardiography (ICG), electrodermal activity (EDA), and continuous blood pressure (cBP). Primary outcomes included efficiency, compliance, tolerability, acceptability, and data quality with progression criteria based on the traffic light (i.e., red, amber, green) approach. Of the 11 subjects, 10 completed the full battery with 1 subject withdrawing due to an unanticipated adverse event. Overall, the results suggested that our battery is feasible with minor changes. Chiropractic intervention trials are currently underway exploring the feasibility of a modified version of this battery in clinical populations.

KEYWORDS

Central Nervous System; Peripheral Nervous System; Autonomic nervous system; Sympathetic Nervous System; Parasympathetic Nervous System; Electroencephalography; Evoked potentials; Electrocardiography; Impedance Cardiography; Chiropractic; Spinal manipulation.

INTRODUCTION

The field of neurophysiology employs an array of well-validated methods to index the activity of both the central and peripheral nervous systems (CNS and PNS, respectively) (1). Importantly, collecting data from both the CNS and PNS in tandem allows researchers to go beyond the evaluation of these systems in isolation and explore potential interactions that are relevant to our understanding of both health and disease.

Beginning with the CNS, the belief that a single brain locus was responsible for any given brain (dys)function pervaded neuroscientific circles for centuries (2, 3). Modern neuroscientists, however, are increasingly embracing a network perspective wherein higher-order cognitions, emotions, and behaviours (i.e., thoughts, feelings, and actions)

emerge from dynamic, hierarchically organised interactions between distributed brain regions. This network approach is rapidly emerging as the most important avenue towards understanding brain (dys)function (4-12). Today, perhaps the most popular approach to investigating human brain networks is in the 'resting state' condition whereby non-invasive neuroimaging (e.g., electroencephalography; EEG) is employed to assess brain activity during periods lacking imposed stimuli or other behaviourally salient events (13). That said, brain (dys)function can also be interrogated via patterned responses to stimuli. Arguably, the most well-known method in this regard is the study of EEG-derived event-related potentials (ERPs) defined as small voltages generated by the brain in response to specific events (14). Assessment of the brain in both resting and non-resting (i.e., stimulus-evoked) conditions holds the promise of providing greater insights into CNS (dys)function (15, 16). Notably, limited data suggests that chiropractic adjustments may modulate CNS functioning in both resting and stimulus-evoked states (16-18).

The CNS is also known to exhibit indirect control of lower-level physiological responses (e.g., heart rate, blood pressure) via modulation of a branch of the PNS known as the autonomic nervous system (ANS) (19). The ANS is divided into the parasympathetic (PSNS) and sympathetic (SNS) nervous systems with the former putatively governing 'rest & digest' functions, and the latter associated with stress-induced 'fight-or-flight' responses (20). There are a wide variety of validated procedures commonly employed to assess PSNS and SNS functioning (21). For example, one of the most recognized surrogate measures of cardiac-related PSNS activity is respiratory-related heart rate variability (HRV) (22-25). Termed respiratory sinus arrhythmia (RSA), chronotropic (i.e., heart rate) changes occur during respiration due predominantly to the modulation of PSNS output at the sinoatrial (SA) node (22-25). As such, non-invasively tracking the heart's *electrical* activity over many respiratory cycles via electrocardiography (ECG) allows researchers to quantify PSNS-mediated HRV, or more precisely heart period (i.e., interbeat interval; IBI) variability, over time (25). Regarding SNS activity, systolic time intervals (STIs; e.g., pre-ejection period; PEP) are well-recognized and validated measures which can be captured using non-invasive techniques such as impedance cardiography (ICG) (25). The SNS exerts inotropic (i.e., heart contraction) effects via the ventricular myocardium (25). ICG allows researchers to track the heart's *mechanical* activity by monitoring electrical impedance changes in the thorax (26). The duration between ECG-derived electrical activity (i.e., onset of left ventricular depolarization; Q-wave) and ICG-derived mechanical activity (i.e., opening of the aortic value; B-point on the dZ/dt trace) is termed the PEP and is a widely recognized method of estimating the degree of cardiac SNS activity (26). Another popular non-invasive method of SNS evaluation is via electrodermal activity (EDA), which measures the electrical fluctuations on the skin modulated by SNS-mediated eccrine sweat gland activity (27).

There may be value in assessing ANS (dys)function across both resting and non-resting (e.g., reactive) conditions (25). A commonly employed example of the latter involves tracking putative SNS-mediated blood pressure (BP) responses to sustained isometric exercise (e.g., isometric handgrip, IHG) (21). A recognized benefit associated with

isometric versus dynamic (e.g., running) exercise is the minimization of body movements which can interfere with the accuracy of hemodynamic measurements (28). Some evidence suggests that chiropractic adjustments may modulate ANS output, at least at rest (29-31). That said, a recent review examining the effectiveness of spinal manipulative therapy (SMT) at modulating ANS activity concluded that high quality studies with rigorous data collection processes are lacking (32). Moreover, we are not aware of any trials that have rigorously investigated potential alterations in ANS responses to stressors, or the relationship between CNS and ANS modulation after receiving chiropractic care or SMT.

Chiropractic is based on the premise that correcting vertebral subluxations will improve central neural function, which in turn will result in improved human performance and potentially clinical outcomes.(33, 34) It has been suggested that vertebral subluxations impact central neural function due to a breakdown in central segmental motor control that results in altered afferent feedback from muscle spindles in the paraspinal muscles at subluxated levels of the spine.(33, 35) This, in turn, is thought to result in maladaptive neural plastic changes in the CNS that can result in altered sensorimotor control, altered whole body motor control, altered ANS control and overall poor health and function.(36, 37). A protocol that employs a robust, evidence-based methodology to assess CNS- and PNS-related outcomes in a variety of conditions can aid the chiropractic profession in the validation of these claims.

Life University's Dr. Sid E. Williams Center for Chiropractic Research (CCR) undertook a study to examine the feasibility of deploying a series of subjective and objective assessments of CNS and PNS (i.e., ANS) functioning under basal (i.e., resting) and reactive conditions. This trial's primary aims surrounded the feasibility of our processes and protocols. More specifically, we wanted to assess our battery with respect to 1) efficiency (i.e., average battery duration), 2) tolerability (i.e., proportion of participants able to complete a given assessment), 3) acceptability (i.e., how acceptable participants rate each aspect of the protocol), 4) data quality (i.e., proportion of test acquisitions with data suitable for subsequent analyses), and 5) adherence (i.e., proportion of participants adhering to the pre-session lifestyle restrictions). Ultimately, this feasibility trial is the first step in the development of an efficient yet comprehensive battery that can be deployed in future clinical trials examining the purported effects of chiropractic/SMT on the nervous system.

METHODS

Study population & setting

The targeted population for this single-arm feasibility trial was healthy adults living in and around Atlanta, Georgia, USA. This study was undertaken at Life University's CCR located in Atlanta, Georgia, USA and was approved by Life University's Institutional

Review Board (IRB) on October 12, 2022. As this was a feasibility study without an intervention, a single arm trial was a cost-effective means of assessing our protocols and procedures.

Eligibility Criteria

The following eligibility criteria were established for this study:

- 18+ years of age.
- Able to speak and read English.
- No impaired function of the dominant hand.
- No malignant hypertension.
- No history of cerebral aneurysms or epilepsy.
- No history of heart conditions, including implanted devices
- No untreated/uncontrolled externalizing or thought disorders.
- No surgeries or serious injuries to the head or torso in the last 3 months.
- No hearing impairments.
- Not pregnant.
- No current litigation related to a physical, health-related injury.

Recruitment

As this was a feasibility study, a small (n=11) convenience sample was recruited. Recruitment took place from October 31 to December 16, 2022. An email was sent out to Life University students and staff containing a digital flyer briefly describing the study along with a link and QR code directing them to a Health Insurance Portability and Accountability Act (HIPAA) protected JotForm screening survey (Jotform Inc., San Fransisco, CA, USA). Paper flyers were also posted on and around Life University's campus. Recruitment materials mentioned receipt of $50 in gift cards (i.e., Amazon, Publix, Uber Eats, Target) plus a $10 gas card for participation. Those who completed the online screen and met the eligibility criteria were contacted via email and scheduled for a single session at the CCR. The email contained directions to the lab and a link to a HIPAA protected JotForm initial research intake sheet (IRIS) which captured basic demographic and clinical information.

Pre-session preparation

Reminder emails were sent to each participant ~24 hours and ~4 hours prior to each appointment. To optimize EEG signal quality, the emails requested that participants wash their hair and refrain from adding any hair products (e.g., gel), braids, and/or hair accessories. Additionally, they were asked to reschedule if they were in any physical pain or overly tired on testing day and abide by certain lifestyle restrictions including abstaining from 1) consuming large quantities of food (i.e., >300 calories) and water (i.e., >350 ml or ~12 oz), alcohol-based mouthwash, nicotine, and caffeine for 4 hours, and 2) strenuous exercise, alcohol, and over-the-counter medications for 24 hours. Adherence to these

pre-session guidelines was queried at the beginning of the session with any breaches recorded. To ensure an empty bladder, participants were instructed to use the toilet immediately prior to testing and avoid washing their hands with soap. Together, these standardisation procedures are in line with current recommendations for neurophysiological data collection (38-40) and designed to control for variability in neurophysiological output stemming from potentially important factors such as the degree of gastric (39, 41, 42) and bladder distention (39, 43), and circulating levels of caffeine (44, 45), nicotine (46, 47), and alcohol (48, 49).

Informed consent & enrollment

Upon arrival at the CCR, participants were briefed on the study protocol (**Fig. 1**), informed of their rights as a participant, and asked to the informed consent document.

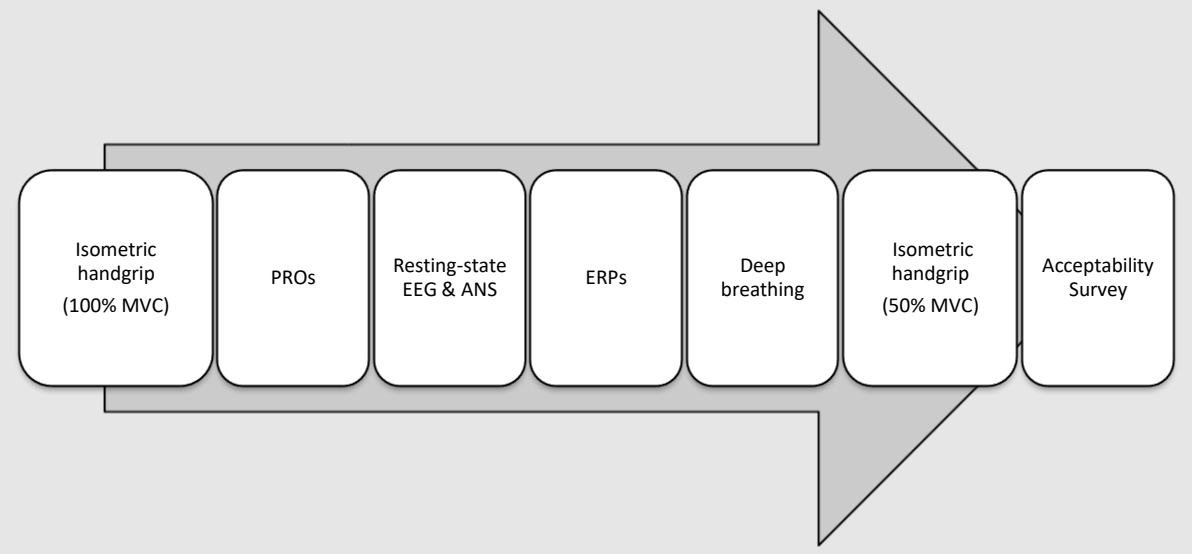

Figure 1: Assessment flow chart; note: MVC = maximum voluntary contraction; PROs = patient reported outcomes; EEG = electroencephalography; ANS = autonomic nervous system; ERPs = Event-related potentials.

Data Collection and Measurements

ISOMETRIC HANDGRIP (IHG): 100% MVC

At least 30-min prior to the resting-state assessments, maximum grip strength was assessed using a Jamar dynamometer fitted with Ultium hand grip dynamometer SmartLead to wirelessly transmit force data (sampling rate: 2000 Hz) to the Noraxon software (version MR 3.18). The dynamometer was calibrated according to the manufacturer's instructions before each measurement. As the dynamometer allows for 5 different grip positions (35-87 mm), the grip position was adjusted to each participant's hand size prior to testing. For testing, participants were instructed to keep their feet flat on the floor, maintain a 90-degree angle at the elbow, and not use the armrest (**Fig. 2**).

Participants performed 3 trials whereby they gripped the dynamometer using maximum force with their dominant hand for ~3 seconds. The average of the three trials was taken as their maximum voluntary contraction (MVC) value. The MVC served as the baseline measure for calculation of the 50% MVC applied in a later assessment.

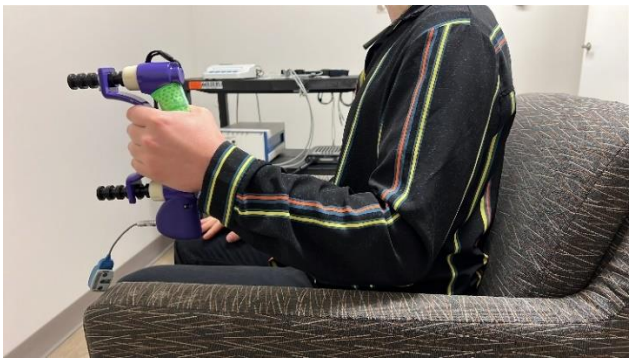

Figure 2: Isometric handgrip challenge.

PATIENT REPORTED OUTCOMES (PROS)

Patient reported outcomes (PROs; English versions) included the 31-item Composite Autonomic Symptom Score (COMPASS-31) (50), 20-item Cognitive Flexibility Inventory (CFI) (51), and the 15-item Mental Fatigue Scale (MFS) (52). Research has shown that electronic data collection increases the speed, accuracy, and user acceptability of the process (53-55), therefore all PROs were re-created in digital form via Jotform and participants were asked to complete the PRO series on a electronic tablet during their EEG/ANS set-up. To prevent missing data, a visual alert was generated if any queries on a given form had missing responses.

In addition, our lab created a digital 14-item post-session survey asking participants to rate from 1 (strongly disagree) to 5 (strongly agree) the acceptability of various aspects of the trial. At the end of the post-session survey, we included a field encouraging additional comments about the procedures and overall experience (see supplement).

RESTING STATE CNS & ANS ASSESSMENTS

RESTING STATE EEG

EEGs were acquired via an FDA approved, CE class IIb certified Neuroscan SynAmps RT amplifier (Compumedics Inc., Charlotte, NC, USA) using a continuous sampling rate of 1000 Hz. Recordings took place in a quiet, comfortable room with participants seated upright in a comfortable chair with their eyes closed. We chose the eyes-closed condition because it has been reported to improve EEG reliability (56, 57). A high-density (64-channel) silicone Quik-Cap Hydro Net with Ag/AgCl electrode placements corresponding

to the international extended 10/20 system was applied to the head (**Fig. 3**). The ground electrode is positioned at AFz with the reference electrode midway between Cz and CPz. A flexible tape measure was used to determine cap sizing (S, M, L, XL). Caps were soaked in a saline solution at least 30-minutes prior to application, and all electrode impedances were kept below 30 kΩ. To help reduce impedances, an appropriately sized Surgilast tubular elastic dressing retainer (Western Medical Ltd., Tenafly, NJ, USA) was placed over the net. An additional electrode was placed on the left sub-orbital region to monitor eye movement, and a chin strap was used to ensure the cap remained secure.

Figure 3: 64-channel Quik-Cap Hydro Net

To improve analysis accuracy, a pair of eye frames (lenses removed) with digital markers attached at the bridge of the nose, near the left ear, and near the right ear were fitted on each participant (**Fig. 4**). Electrode positions and fiducials were digitized using the Polhemus Fastrak (Polhemus Inc., Colchester, VT, USA) and Curry 8 software (version 8.0.6S). A stylus was used to record the exact location of the tragus of the left ear, the tragus of the right ear, and each of the 64 EEG electrodes. Once all locations were digitized, the frames were removed. During the ~6-minute acquisitions, participants were asked to place their arms in their laps with their palms facing up and remain quiet and still for the duration.

Figure 4: Frames with digital markers (left), stylus (center), and digitized locations (right)

RESTING STATE ANS

During the resting-state EEG, ANS-related signals (i.e., EDA, ECG, ICG, respiration) were acquired with Ag/AgCl spot electrodes at a 1000 Hz sampling rate using the AC-coupled, 8-slot Mindware BioNex amplifier (Mindware Technologies Ltd., Gahanna, OH, USA) and Biolab software (version 3.4.1).

For EDA, 1.5" x 1" rectangular foam electrodes were secured to the middle phalanges of the index and middle fingers of the participant's non-dominant hand (**Fig 5;** configuration 2). The non-dominant hand was chosen to prevent artifact during the isometric handgrip (IHG) challenge which is performed with the dominant hand. The areas were prepared by wiping the skin with a wet paper towel, allowing the skin to dry, and applying disposable adhesive electrodes (0.5% chloride wet gel). A continuous, low voltage (0.5V), direct current (DC) was sent between the electrodes to measure the resultant current flow and derive skin conductance.

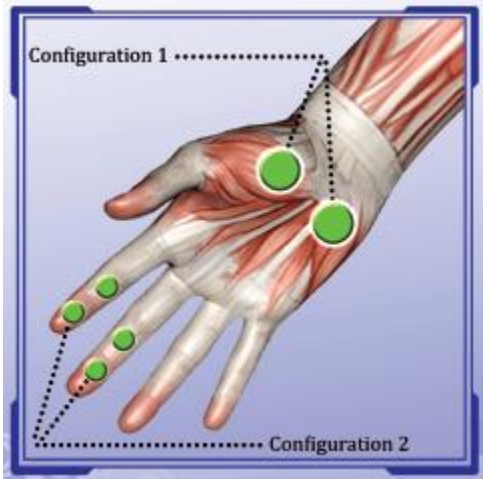

Figure 5: EDA acquisition configurations *(reproduced with permission from Mindware Technologies LTD)*

Participants were asked to lift their arms and a Mindware *modified* piezo-electric respiration belt was wrapped around their torso approximately at the level of the diaphragm. This belt contains a piezo-electric device that responds linearly to changes in length. The belt was tightened to allow just enough room for two fingers to fit snuggly between the belt and the thorax.

If needed, participants were asked to shave any areas on the thorax where the 1.5" circular foam ECG/ICG electrodes (7% chloride wet gel) were to be applied. A research assistant prepared each area by rubbing an alcohol wipe a circular motion until the skin was slightly abraded and red. The ground electrode was attached at the level of the 12th rib on the right antero-lateral thorax. A small piece of medical tape was used to create a strain relief loop in each electrode lead wire just proximal to the electrode.

To track the heart's electrical activity, we used a standard lead-II ECG with the negative electrode on the right clavicle and the positive electrode at the level of the 12th rib on the

participant's left antero-lateral thorax (**Fig. 6**). To track the heart's mechanical functioning, two ICG sensing electrodes were secured to the anterior thorax with the negative electrode at the xiphoid process and the positive electrode on the sternal notch (**Fig. 7**). The distance between these electrodes was measured (in cm) and recorded. Two ICG constant current source electrodes were then attached to the posterior thorax with the positive electrode near the inferior aspect of the cervical spine (~4 cm superior to the sternal notch level) and the negative electrode near the inferior aspect of the thoracic spine (~4 cm inferior to the xiphoid level). A continuous, high-frequency (100 kHz), low-amplitude (500 µA), alternating current (AC) was passed through the thoracic cavity to quantify impedance levels. The magnitude of the 100 kHz signal received by the sensing electrodes was displayed as the raw impedance waveform (Z_0). Additionally, the first derivative of Z_0 (i.e., dZ/dt) was displayed and recorded.

All leads were then inserted into the Bionex amplifier and visual checks of each signal were performed to ensure proper polarity and a high signal-to-noise ratio prior to acquisitions. During the ~6-minute acquisitions, participants were asked to close their eyes, place their arms in their laps with their palms facing up, and remain motionless and quiet.

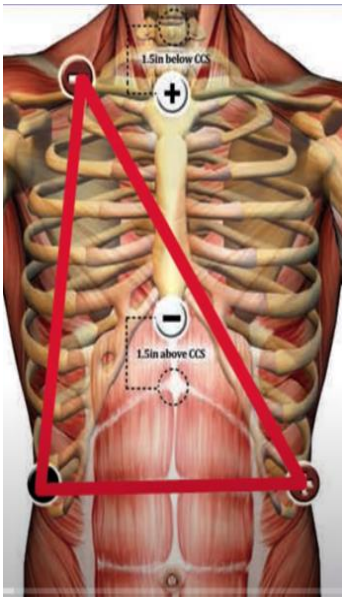

Figure 6: ECG lead-II configuration shown by the red triangle *(reproduced with permission from Mindware Technologies Ltd.)*

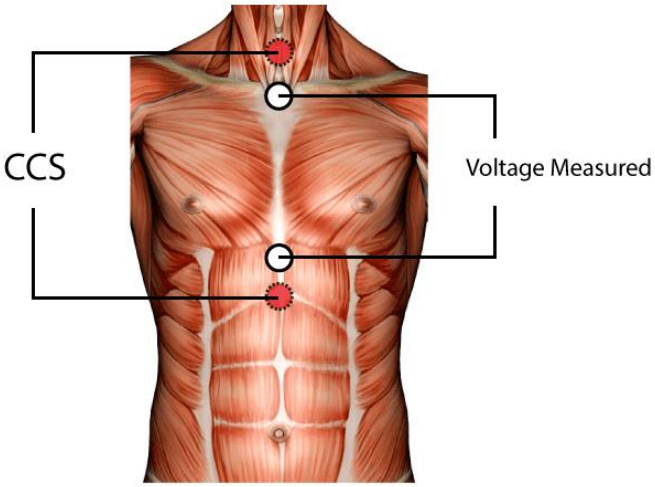

Figure 7: ICG electrode configuration showing constant current source (red dots) and sensing (white dots) electrodes *(reproduced with permission from Mindware Technologies Ltd.)*

NON-RESTING STATE CNS & ANS ASSESSMENTS

EVENT RELATED POTENTIALS (ERPS)

Cognitive functioning was assessed using an auditory oddball paradigm with two distinct, randomized stimuli. The standard stimulus was a 1,000 Hz tone (probability = 0.80), and the target stimulus was a 2,000 Hz tone (probability = 0.20). The tones were presented using E-Prime v3.0 software with Chronos box (Psychology Software Tools, Pittsburgh, PA, USA) and noise-isolating earphones (Etymotic ER-4B MicroPro, Elk Grove Village, IL, USA). Stimulus presentation duration was set at 200 ms, and the interstimulus interval was 1500 ms. With eyes closed, participants were instructed to respond as quickly and accurately only to the target stimuli by pressing a button on the Chronos box each time they heard the target. The Chronos box was positioned on a table at a comfortable distance to the participant's dominant hand. Stimulus events and behavioral responses were recorded using the E-Prime 3.0 software. Prior to the test trial, participants were presented with both stimuli to ensure they could hear and distinguish between the different tones.

DEEP BREATHING

A popular method of quantifying RSA is the peak-to-trough method (59). For this, we collected a 60-sec, paced-breathing ECG from each participant using a free digital metronome application (version 1.0; Metro Timer). During pacing, participants were instructed to perform a series of six slow, maximal inhalations and exhalations through their nose using a 1:1 inspiratory/expiratory ratio (i.e., 5 sec inspiration/5 sec expiration).

ISOMETRIC HANDGRIP (IHG): 50% MVC

Continuous, non-invasive monitoring of beat-by beat BP (cBP) was performed during a sustained IHG contraction. An FDA cleared, CE class II certified Caretaker 4 wireless vital signs monitor (sampling rate 128 Hz; Caretaker Medical, Charlottesville, VA, USA) was secured to the wrist of the participant's non-dominant hand using an adjustable wrist cuff. Pulse pressure was continuously monitored via an adjustable finger cuff attached to the middle phalanx of middle finger with the bladder facing the palm, and then connected to the vital signs monitor via an air hose. Once the connection was secure, the monitor was turned on. Following a minimum 5-minute seated rest period, a baseline BP was measured with the OMRON IntelliSense Professional Digital BP Monitor and upper arm cuff (model HEM-908XL; OMRON Healthcare Inc., Lake Forest, IL, USA). The vital signs monitor was paired via Bluetooth to a digital tablet running the Caretaker 4 software application (version 1.6.37), and the baseline BP was manually entered into the software to calibrate the unit. The equipment and set up are shown in **Fig. 7**.

Figure 7: Caretaker 4 equipment (i.e., wireless wrist monitor, finger cuff, tablet) and set up.

For the sustained IHG assessment, participants were told to keep their feet flat on the floor, maintain a 90-degree angle at the elbow, and not use the armrest. Additionally, they were instructed to verbally count from '0' during the effort to avoid breath holding (i.e., a

Valsalva maneuver). Using their dominant hand, they were asked to perform a single 2-min IHG at 50% MVC on the dynamometer. A computer monitor was positioned in front of the participant which displayed the target force and continuous, real-time visual feedback of their force production during the effort. After 2-min, they were asked to cease gripping, and the dynamometer was removed.

Data Processing and Analysis

PROS

PRO data collected via JotForm was exported into Excel 365.

RESTING STATE CNS & ANS ASSESSMENTS

RESTING STATE EEG

Resting state EEG pre-processing was performed offline using freely available EEGLAB software (version 2023.0) running on a MATLAB platform (version 2022a; MathWorks Inc., Natick, MA, USA). A custom script was developed in MATLAB utilizing EEGLAB and MATLAB functions to batch import the raw Curry (.cdt) files into EEGLAB along with their digitized electrode locations using the Neuroscan Curry import plugin, isolate the initial 5-min of resting-state EEG data, and save the EEGLAB (.set) files in a designated folder for subsequent cleaning. Non-brain related artifacts (e.g., muscle activity, line noise) were removed using an automated, freely available software implemented in EEGLAB known as RELAX (Reduction of Electroencephalographic Artifacts; beta version 1.1.4) (60). Briefly, RELAX employs a multi-stage process using EEGLAB (61), fieldtrip (62), and PREP (63) functions implemented in MATLAB to 1) remove extreme outlying channels and time periods from raw, continuous, multi-channel EEG data, 2) perform three consecutive runs of multi-channel Wiener filtering (MWF) (64) to subtract muscle activity and eye movements, 3) re-reference the data to the robust common average which recalculates the reference signal by averaging the signals from all electrodes (63), and 4) reduce artifactual independent components (ICs) via wavelet enhanced independent component analysis (wICA) (65) applied to artifacts identified by the machine learning algorithm ICLabel (66) all while preserving the neural signal (i.e., not overcleaning the data) (60). RELAX outputs cleaned, continuous, robust average re-referenced, interpolated data that can then be epoched and (if needed) cleaned further prior to analysis (60).

For resting state EEGs, prior to implementing RELAX's phase 1 cleaning cycle, we removed unwanted channels (REF, TRIGGER, EKG, EMG, HEOG, VEOG, M1, M2, CB1, CB2, FT11, FT12), bandpass (4^{th} order acausal Butterworth, 1-80 Hz) and notch (2^{nd} order acausal Butterworth, 60 Hz) filtered the data, and down sampled the signal to 500 Hz for faster independent component analysis (ICA) processing. Of note, the deleted

channels are considered to be non-scalp electrodes which are recommended to be removed by the developers of RELAX (60). Adaptive mixture ICA (AMICA) (67) was selected as it has been shown empirically to outperform other ICA algorithms (68). In phase 2 of RELAX, we interpolated rejected channels, segmented the data into 2 second epochs, and removed epochs that exceeded our rejection thresholds. Following each phase of RELAX, data quality checks were performed via inspection of the cleaning metrics output by RELAX (see supplement **Table 1S**). The specific phase 1 and 2 parameter settings that were chosen within the RELAX graphical user interface (GUI) are detailed in the supplement (**Fig. 1S** & **2S**). A flow chart of the resting-state EEG pre-processing pipeline is depicted in **Fig. 8**.

Figure 8: Resting-state EEG pre-processing pipeline.

RESTING STATE ANS

Resting state ANS signal processing was performed offline using freely available Biolab software (version 3.4.1; https://support.mindwaretech.com/downloads/) and proprietary Autonomic Nervous System Laboratory Professional software (ANSLAB; version 2.6) (69) running on MATLAB 2022a. ANSLAB is a software suite that permits data visualization, artifact detection, data reduction, and statistical analysis for a wide range of ANS-related signals.

Raw Mindware (.mwi) files were individually loaded into Biolab, the initial 5-min of the resting state data was isolated, and the files were exported in ASCII (.txt) format. Each ASCII file contained the sampling rate, tab-delimited column names, and tab-delimited data for each column.

The raw respiration signal was down sampled (25 Hz), bandpass filtered (0.033-1 Hz), and loaded into the respiration module. ANSLAB's algorithm automatically detects and labels four elements of each respiration cycle: 1) inspiration onset, 2) inspiration end, 3) expiration onset, 4) expiration end (see supplement **Fig. 4S**). Each time-series was visually inspected and, when necessary, respiratory cycles were manually labeled (if missed by the algorithm) and/or removed (if noise was misidentified as a respiratory cycle). After editing, the reduced (i.e., respiratory rate) time-series was saved in MATLAB (.m) format at 4 Hz resolution. The reduced time-series was then loaded into ANSLAB's spectral module. This module automatically calculates the average respiratory rate across the acquisition period. Our respiratory range of interest (i.e., ~0.12-0.5 Hz or ~7-30 cycles per minute) was selected based upon the established lower and upper bounds for valid assessments of RSA in adults (70, 71). Any participants with average respiratory rates outside of this range were flagged, and their data was deemed ineligible for subsequent RSA analysis.

Each raw ECG time-series was bandpass filtered (0.5-40 Hz) and loaded into the ECG module. ANSLAB's proprietary algorithm automatically detects and labels R-peaks (see supplement **Fig. 5S**). The ECG time-series was visually inspected and, when necessary, manually labeled (if an R-peak was missed by the algorithm) and/or de-artifacted (if noise was misidentified as an R-peak or an ectopic beat was labelled). In cases of the latter, linear interpolation was often required. Of note, any data files with >10% interpolated R-peaks were flagged and deemed ineligible for subsequent HRV analysis. After editing, the reduced (i.e., IBI) time-series (72). Via a custom script developed in MATLAB, participant values from the metrics of interest (e.g., high-frequency HRV; HF-HRV) were exported to Excel.

Timing files were manually created within the study's "raw" folder for each ASCII file which segmented the ICG signal into 30-second non-overlapping epochs allowing segment-wise analysis and averaging of PEP values. This segmentation was done to help mitigate the potential for B-point "wash out" (i.e., unidentifiable B-points) due to non-stationary signals. Each ICG time-series was then high pass (1 Hz) and notch (60 Hz) filtered and loaded along with its associated timing file (e.g., nbs00101.icg.m) into the ICG module.

Synchronized by the peak of the ECG Q-point (beat-by-beat detection, backward search window = 100 msec, ratio of slope = 0.2), median ensemble averaging of dZ/dt waveforms) was performed on all 30 second segments meeting the minimum threshold of 15 valid beats (see supplement **Fig. 6S**). Per ANSLAB's default parameters (69), waveforms > +/- 2 standard deviations from the mean in the B-point window were considered outliers and automatically excluded. For each ensemble, ANSLAB labeled the B-point, Z-point, and X-point along with their standard error margins within their respective search windows. Due to inter-individual waveform variability (i.e., fidelity and depth of the B-wave), the B-point detection sensitivity and search window positions were manually adjusted for each participant to optimize detection and applied across all segments. The B-point detection algorithm was set to 'notch' which defaults to 'zero-crossing' if ANSLAB is unable to detect a valid B-point. Notably, we ensured that the same algorithm was applied across all valid segments for a given participant. Each ensemble-averaged waveform was visually inspected and, if necessary, B-points were manually adjusted or waveforms without valid B-points were rejected. Once the B-point for all valid ensembles had been established and accepted, the PEP (msec) for each was automatically derived by ANSLAB. These values were saved in MATLAB (.mat) format to the trial's auto-generated 'icg' folder. Via a custom script developed in MATLAB, segment-wise PEP values for each participant were exported to Excel.

Each raw EDA time-series was down sampled to 25 Hz and loaded into the EDA module. The threshold for the detection and identification of non-specific skin conduction responses (NSFs) was set at >0.05 micro-Siemens (μS). The skin conductance level (SCL, in μS) and identified NSF onsets (red dots) were plotted above the raw respiration signal to assist with the identification of artifacts due to abnormal respiratory activity (e.g., sighs) (see supplement **Figure 7S**). Additionally, two bivariate plots of NSF characteristics are displayed to help with the identification of outlier NSFs that may represent motion or technical artifacts. Of note, typical NSFs have a maximum amplitude of 2-3 μS (73). Each EDA time-series was visually inspected. Typical SCL amplitudes range between 1 - 40 μS (73), therefore files with amplitudes <1 μS were flagged and deemed ineligible for subsequent analysis. When necessary, NSFs were manually labeled (if missed by the algorithm) and/or unlabeled (if noise was misidentified as an NSF). Additionally, smoothing was employed in cases of severe artifact that impacted SCL levels. After editing, the reduced (i.e., SCL and NSF rate) time-series data was saved in MATLAB (.m) format at 4 Hz resolution to ANSLAB's 'eda' folder. Via custom script developed in MATLAB, SCL and NSF rate values for each participant were exported to Excel.

Following subject-level inspection of resting-state ANS signals, a final group-level data quality check was performed. Via the ANSLAB GUI, a MATLAB (.m) formatted group-level batch file was created from the raw ASCII files. Group-level batch plots were then created for each edited signal and associated variable(s) of interest to allow for the identification of potential outliers (see supplement **Fig. 8S**). The edited data files of potential outliers were manually re-inspected and, if necessary, rejected.

NON-RESTING STATE CNS & ANS ASSESSMENTS

ERPS

For ERP data, trials with improbable or incorrect behavioral responses or reaction times were removed from analysis. Visual inspection of a reaction time histogram of target trials yielded a probable reaction time range of 180-900 ms for the auditory oddball task. Trials with no reaction time were considered incorrect. Files with more than 50% of the trials considered improbable or incorrect were not included in further analysis. Remaining ERP files were imported into EEGLAB using the Neuroscan Curry import plugin and saved in the EEGLAB (.set) format. Data files were trimmed prior to implementing RELAX Phase 1 to contain no more than 10 seconds prior to the first stimulus presentation and after the last stimulus presentation, unwanted channels were removed (REF, TRIGGER, EKG, EMG, HEOG, VEOG, M1, M2, CB1, CB2, FT11, FT12), bandpass (4^{th} order acausal Butterworth, 0.25-80 Hz) and notch (2^{nd} order acausal Butterworth, 60 Hz) filters were applied, and data was down sampled to 256 Hz. AMICA was chosen for the ICA processing, and channel interpolation occurred after Phase 1. The specific phase 1 parameter settings that were chosen within the RELAX GUI are shown in the supplement (**Fig. 3S**).

Following phase 1 of RELAX, data quality checks were performed via inspection of the cleaning metrics output by RELAX (see supplement **Table 1S**). ERP files were further pre-processed utilizing a custom script using EEGLAB and ERPLAB (74) toolboxes. In line with current recommendations(75), continuous data were segmented into epochs (-200 ms to +800 ms) relative to stimulus onset and baseline corrected. Artifacts were flagged and rejected using ERPLAB's simple voltage threshold function, with the threshold set at 100 μV and ERPLAB's moving window peak-to-peak function, with a window size of 1000 ms, a step size of 100 ms, and a threshold of 100 μV. The entire epoch was excluded if an artifact was flagged on any channel. If an EEG data file contained <75% of the original number epochs for both the standard and target stimuli, then the average ERP for each stimulus type was not computed for that file. Following artifact rejection, a stimulus-locked P300 average was calculated for targets and standards. A flow chart of the ERP pre-processing pipeline is depicted in **Fig. 9**.

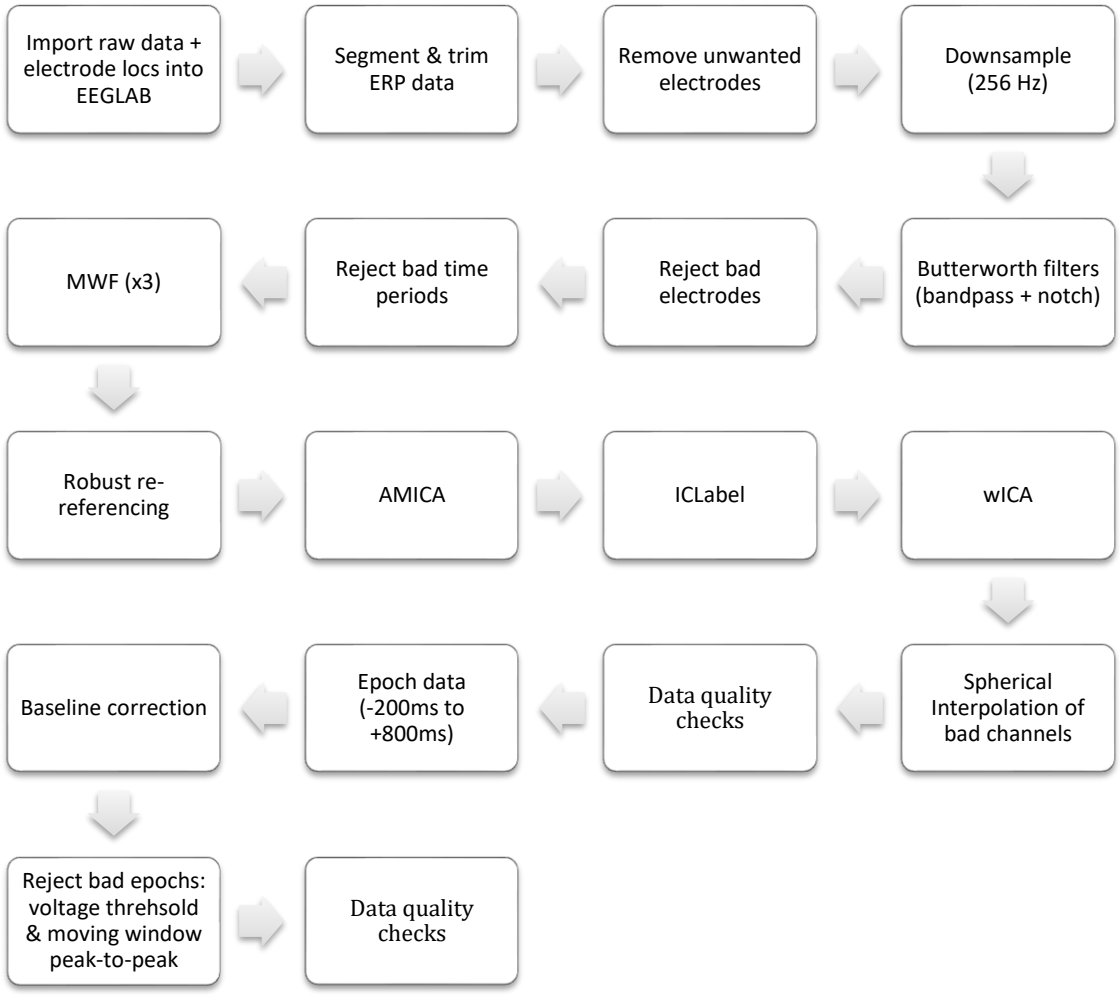

Figure 9: Event-related potential (ERP) cleaning pipeline.

DEEP BREATHING

Raw ECG files collected during deep breathing were individually loaded into Mindware's proprietary Heart Rate Variability Analysis software application (HRV-A; version 3.2.13). HRV-A applies a bandpass filter (0.5-45 Hz, 2nd order Butterworth) to each raw ECG time-series and uses the Shannon's Energy Envelope algorithm (76) to automatically detect and label R-peaks. Additionally, HRV-A utilizes two artifact detection algorithms: 1) IBI min/max (min = 40 bpm, max = 200 bpm,) and 2) MAD/MED (Minimum Artifact Deviation/Maximum Expected Deviation (77)). Each ECG time-series was visually inspected and, when needed, manually labeled (if an R-peak was missed by the algorithm) and/or de-artifacted (if noise or an ectopic beat was labelled). When

necessary, the HRV-A midbeat interpolation function was employed. Of note, any data files with >10% interpolated R-peaks were flagged and deemed ineligible for subsequent analysis. For retained data files, all IBIs for each respiratory cycle were segmented and exported to Excel for subsequent computation of the metric of interest (i.e., expiratory/inspiratory (E/I) ratio which is defined as the longest IBI/shortest IBI averaged across the 6 respiratory cycles).

IHG

For cBP data processing, the Caretaker 4 tablet was connected to the laptop and participant files were transferred to a designated study folder in Excel format. Data is then converted to CSV format and exported to Biopac's proprietary Acknowledge software (v5; Biopac Systems Inc., Goleta, CA, USA) for subsequent signal visualization and editing. The systolic and diastolic peaks within the pulse pressure waveform are identified using the software's automated peak detection function. If needed, artifacts are removed, peaks are manually identified, and interpolation of peaks is performed. Of note, any data files with >10% interpolated peaks are flagged and deemed ineligible for subsequent analysis. Following editing, calculations are then performed to derive the metrics of interest. Specifically, we are interested in the estimated maximum diastolic BP (dBP), systolic BP (sBP), and mean arterial pressure (MAP) excursion from a 2-min averaged baseline during the IHG challenge.

A summary of data quality checks used in our ANS pre-processing pipeline are provided in the supplement (**Table 2S**).

Primary outcomes

A list of implementation outcomes and progression criteria is provided below (**Table 1**). For the progression criteria, we chose the traffic light (i.e., red, amber, green) approach (78). The outcomes and criteria were drafted following several rounds of discussions and informed by existing literature and trialists' experience.

Table 1: Implementation outcomes & progression criteria.

	Green/Go: Feasible without changes	Amber/Caution: Feasible with minor changes	Red/Stop: Feasible with major changes or infeasible
Efficiency: Average battery duration	≤90 min	>90 & ≤120 min	>120 min
Compliance: % of participants violating 1 or more pre-session lifestyle restrictions	≤10%	>10% & ≤20%	>20%
Tolerability:	≤10%	>10% & ≤20%	>20%

% of participants unable or unwilling to complete a given assessment			
Data quality: % of acquisitions from a given assessment unsuitable for analysis	≤15%	>15% & ≤25%	>25%
Acceptability: % of participants scoring ≤3 in each domain	≤10%	>10% & ≤20%	>20%

RESULTS

Enrollment

As shown in the CONSORT flow diagram (79) (**Fig. 10**), of the 42 subjects who completed the online screening survey, 5 were excluded for not meeting the eligibility criteria. The remaining 37 potential participants were invited to participate via email; however, 26 were non-responsive. Ultimately, 11 individuals were scheduled, consented, and enrolled.

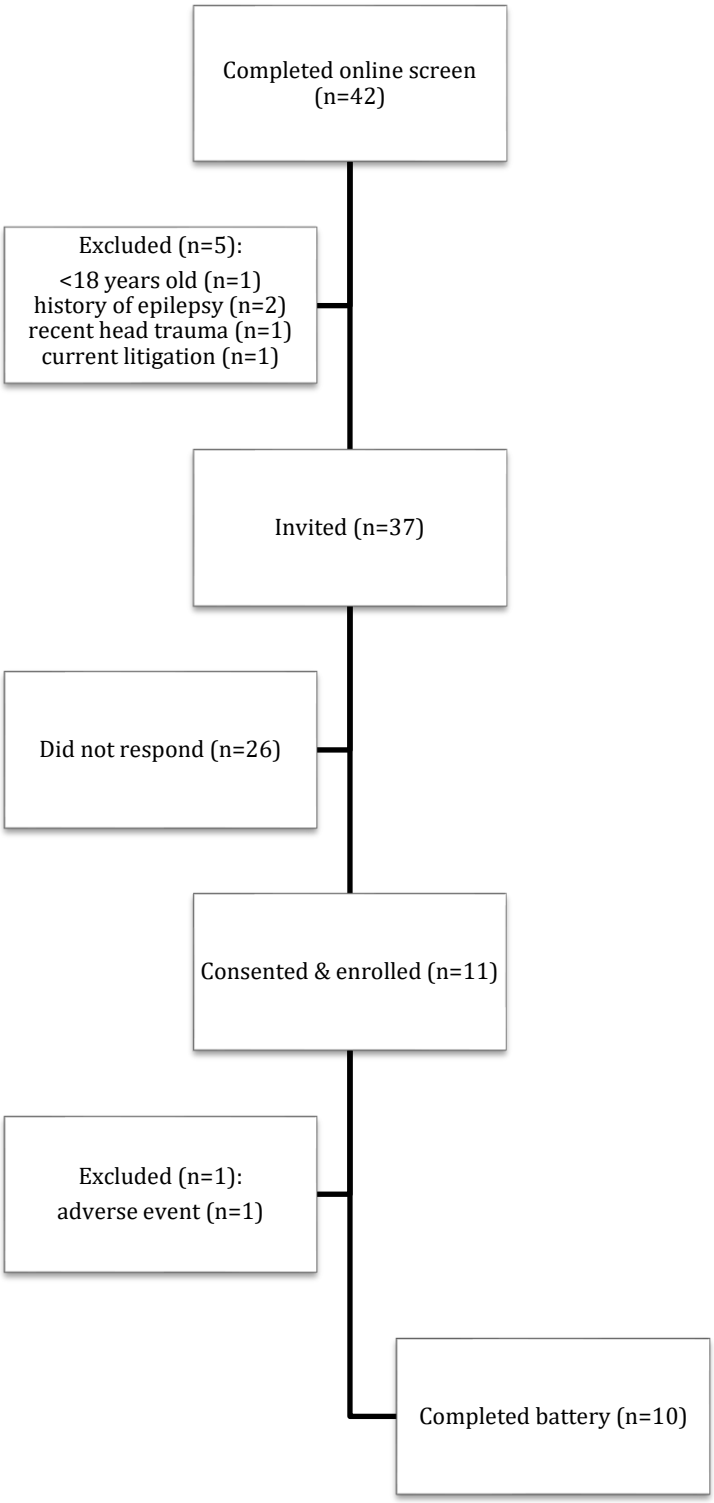

Figure 10: CONSORT Flow diagram.

Demographic and clinical information

Due to a technical issue within Jotform, demographic and clinical data collected through the electronic health history form was irretrievable.

Efficiency

Our 'green light' criterion was met for efficiency. Battery duration was defined as the time (in minutes) from the initiation of the pre-session compliance queries to the submission of the post-session acceptability survey. The mean (±SD) for the battery was 83 (±12) min.

Compliance

The 'green light' compliance criterion was met for most lifestyle restrictions. None of the participants (0%) breached the 24-hour lifestyle rules, which involved refraining from alcohol, intense physical activity, and over-the-counter medications. Similarly, 0 out of 11 (0%) violated the 4-hour restrictions concerning the consumption of caffeine, nicotine, alcohol-infused mouthwash, and substantial amounts of food. That said, water intake met the 'red light' criterion. Specifically, 4 out of 11 (36%) failed to adhere to the limits on water intake, with three participants drinking 16 oz and one participant drinking 48 oz of water in the 4-hour period before their testing sessions.

Tolerability

All aspects of the battery met the 'green light' tolerability criterion. All 11 participants (100%) were able to complete the PROs on the digital tablet during EEG set up. Notably, 1 participant (9%) was unable to complete the assessment battery due to severe discoloration of the middle finger shortly following the application of the cBP finger cuff. Subsequent resting-state EEG/ANS, ERP, deep breathing, and IHG at 50% MVC assessments were well tolerated and completed by 10 of 11 (91%) enrolled participants.

Data quality

With respect to data quality, most acquisitions fell within the 'green light' criterion. Firstly, complete data from all 3 PROs (i.e., CFI, MFS, COMPASS-31) was submitted by 11 of 11 enrolled participants (100%) and deemed suitable for analysis. Out of 10 resting-state EEG files, 9 (90%) were retained and considered suitable for subsequent analysis following our pre-processing pipeline. Per our guidelines, 1 acquisition (10%) was deemed unsuitable because the number of electrodes rejected following phase 1 of RELAX exceeded our 25% threshold. With respect to resting-state ANS acquisitions, no respiratory files (0%) were flagged as the respiratory rates for all participants fell within the typical adult range (i.e., ~0.12 to 0.5 Hz or ~7 to 30 cycles per min) which is required for valid RSA analysis. Similarly, 0 of 10 ECGs (0%) and 0 of 10 ICGs (0%) were rejected. Of note, 3 ICG files had a small number of 30-sec segments removed due to either a lack

of an identifiable B-point or failing to meet the threshold of 15 valid beats; however, because the PEP for a given participant is averaged across segments, these files were retained and deemed eligible for subsequent analysis. Out of 10 ERP recordings, 9 (90%) were included in the final analysis. One file was rejected because 50% of the test trials were considered improbable or incorrect based on the visual inspection of the corresponding behavioral response data. Lastly, for the deep breathing task, none of the 10 ECG files (0%) were rejected. That said, 2 signals met our 'red light" criterion. Namely, 10 of 10 EDA files (100%) were rejected due to SCL amplitudes falling 1-2 orders of magnitude below the 1 μS threshold. Similarly, while IHG (50% MVC) cBP data was acquired from all participants, all 10 files (100%) had to be discarded. This was due to the fact that the exported cBP data was batched with values computed as 60-second segment averages by Caretaker 4 prohibiting offline signal processing and the evaluation of the maximum excursion from the baseline.

Acceptability

Of the 14 survey items assessed, 13 items fell within the 'green light' acceptability criterion. Specifically, 12 of 13 received a '4' or '5' rating from all 10 (100%) of the participants. For item 10, which was concerned the ability to hold a steady grip for 2 minutes, 9 out of 10 participants (90%) gave an acceptability rating of '4' or '5', with a single participant (10%) rating it a '3'. Item 2, which dealt with the ease of adhering to pre-appointment guidelines 24 hours and 4 hours prior to the appointment, met the 'yellow light' criterion with 8 out of 10 participants (80%) rating the acceptability as '4' or '5' while 2 subjects (20%) provided a rating of '3'.

DISCUSSION

In trials involving chiropractic/SMT, there is a well-recognized need for more robust designs that employ methodologically sound neurophysiological data collection and processing procedures (32). Here, we endeavored to take the first step in the development of an efficient and robust battery that assesses CNS and PNS function across conditions (i.e., resting and non-resting states) that could be deployed in studies investigating the neurophysiological effects of chiropractic/SMT. Our results suggest that our procedures and protocols are feasible albeit with minor modifications.

Encouragingly, our efficiency target of ≤90 minutes was met with a mean battery duration of 83 minutes. In fact, the longest battery duration only exceeded this target by 15 minutes. Of note, EEG set up time was extended during this study due to a minor technical issue (i.e., elevated impedance values in select EEG electrodes) that has since been remedied (i.e., faulty electrodes removed and replaced). Additionally, prior to sessions we now ensure that all electrodes are functioning via displaying proper impedance values (<1 kΩ) while immersed in saline solution.

Regarding compliance, nearly all pre-session lifestyle restrictions appeared feasible without modifications. The notable exception was limited water intake (i.e., <350ml or ~12 oz in the 4 hours prior to testing), a condition that was violated by ~36% of enrolled

participants. The primary concern surrounding the ingestion of liquids is related to the modulation of neurophysiological signals due to significant gastric (39, 42) and/or bladder distention (39, 43); however, daily water requirements display wide inter-individual variability and are dependent on factors such as sex, body size, and activity levels (80). With these considerations in mind, we believe our requirements were too stringent and have since modified our guidance to permit ab libitum water consumption while still prohibiting rapid ingestion of large quantities (e.g., chugging a 16 oz bottle of water) in the 3 hours immediately preceding testing. We believe this modification, along with bladder emptying immediately prior to testing, will mitigate potential issues related to gastric and/or bladder distention as well as dehydration. Of note, although there were no obvious violations of food ingestion (i.e., consuming >300 calories in the 4 hours prior to testing), this was difficult to confirm as self-reported intake responses varied from “none” to “oatmeal” to “fruit and yogurt”. Like liquids, food ingestion will increase gastric distention and influence neurophysiological activity (38, 39). As such, we now ask participants to abstain from any food ingestion within the 3-hour window immediately prior to testing; however, to help prevent issues related to hunger/satiety, we provide a small, standardized snack upon arrival at the lab. It should be mentioned that to reduce the burden and complexity for participants, the window of caffeine, nicotine, and alcohol-based mouthwash abstinence has also been shortened to 3 hours.

Regarding tolerability, PRO acquisition during EEG set up seemed to be well tolerated by all participants. Saline solution from the electrodes occasionally dripped into participants’ eyes requiring them to utilize the towel provided and momentarily taking their focus from the tablet; however, this minor inconvenience and is unlikely to have impacted data quality and does not appear to have been an issue for participants as evidenced by a lack of acknowledgement in the open-ended response field of the post-session surveys. Similarly, all neurophysiological assessments (resting-state EEG/ANS, ERPs, deep breathing, IHG) were deemed tolerable as they were completed by 10 (91%) of enrolled participants. Of note, one participant failed to attempt these assessments because they experienced circulation issues shortly after the inflation of the finger cuff used for cBP acquisition. Following the incident, this individual reported to the research staff that they suffered from Raynaud’s phenomenon, a condition characterized by vasospasms within the digits following cold, emotional, or physical stressors (81, 82). Due to the unanticipated loss of demographic and clinical data, we were unable to confirm whether this had been reported prior to testing. In any case, we immediately informed the IRB of the incident and would caution investigators on the inclusion of participants with Raynaud’s when incorporating cBP assessments utilizing finger cuffs. Our lab will be mindful of this population in future trials.

Data quality targets were met for all subjective and neurophysiological outcomes with two notable exceptions: 1) resting-state EDA and 2) cBP during IHG at 50% MVC. Firstly, off-line analysis of EDA signals clearly indicated that SCLs were orders of magnitude below putative normative SCLs (i.e., >1-2 μS) (73). Unfortunately, this prohibited analyses of SCLs and NSFs. Subsequent internal testing revealed that the manufacturer likely applied insufficient quantities of 0.5% chloride wet gel to the EDA sensors as the application of

additional gel allowed for normative levels to be attained. As such, we now apply 0.5% chloride gel to all EDA sensors and verify normative SCLs prior to acquisitions. Secondly, the data export limitations for cBP effectively rendered the use of the Caretaker 4 equipment during the IHG challenge infeasible. As such, we have modified our outcome measures and are now assessing HRV and PEP reactivity via ECG and ICG tracking during the IHG challenge. This modification provides several benefits including: 1) reduced participant burden due to a reduction in the amount of attached hardware and time required for calibration, 2) reduced number of eligibility criteria (i.e., Raynaud's not excluded), and 3) allowing for the simultaneous assessment of SNS- *and* PSNS-related modulation via PEP and HRV changes, respectively.

Of the 14 items assessed for acceptability, 13 met our 'green light' criteria. The sole exception was the ease of adhering to lifestyle restrictions. The two participants who rated the acceptability of this aspect of the protocol relatively low (i.e., '3') confirmed their compliance with all pre-session rules; however, one indicated that they found the water restrictions particularly hard to follow as their usual consumption during a 4-hour period is significantly higher. As mentioned, we have since eased our restrictions by permitting ad libitum water intake while still prohibiting rapid ingestion and reducing the food, nicotine, caffeine, and alcohol-based mouthwash abstinence period to 3 hours. These amendments allow us address acceptability concerns in this domain while still conforming to 'best practice' guidelines (38-40). Of note, two additional subjects indicated in their post-session surveys that the lifestyle restrictions detailed in the ~24-hour pre-session email were unanticipated. This was an oversight on our part, and we have taken steps to remedy this issue by ensuring that these requirements are clearly outlined in initial communications with potential participants.

LIMITATIONS

One of the key limitations of our feasibility study was its small sample size which was imposed to limit resource (i.e., time and financial) expenditures. It has been acknowledged that in some circumstances relatively large sample sizes may be needed to uncover issues related to certain process (i.e., implementation) outcomes (83). Further, the generalizability to the wider adult population is limited as this was a convenience sample of healthy individuals recruited in and around the university. To recruit a sample more representative of the general population, future trials will employ wider community outreach efforts such as social media and newspaper marketing. The loss demographic data was also a major limitation. In response, we have modified our data backup protocol. We now perform weekly digital backups as well as redundant backups in digital format and on flash drives. Another potential limitation of our current design is the presence of order effects which can influence outcomes (84, 85). To address this, future designs will consider approaches like mixed effect models which allow for statistical control of order effects by including them as a fixed effect (86). Finally, our resting-state EEG and ANS data acquisitions utilized separate amplifiers and were not precisely synchronized which limits our ability to do advanced analyses of time-locked CNS-PNS interactions (e.g., heart-brain dynamics (87)). In recognition of this shortcoming, our lab has modified its

protocol whereby resting-state CNS and ANS (i.e., ECG) signals are now acquired from a single amplifier.

CONCLUSION

Overall, we found that our protocols and procedures were feasible with relatively minor changes per our established criteria. The results of this study have been instrumental in guiding our efforts to further refine our neurological assessment battery which has recently been expanded to include somatomotor function. We intend to introduce this expanded battery in future feasibility and pilot trials using more robust methodologies (e.g., longitudinal design, addition of control and treatment groups, blinding of outcome assessors) as we seek to comprehensively assess the potential neurophysiological effects of chiropractic/SMT in a wide variety of clinical populations.

REFERENCES

1. Luhmann HJ. Neurophysiology. In: Runehov ALC, Oviedo L, editors. Encyclopedia of Sciences and Religions. Dordrecht: Springer Netherlands; 2013. p. 1497-500.

2. Fornito A, Zalesky A, Breakspear M. The connectomics of brain disorders. Nature reviews Neuroscience. 2015;16(3):159.

3. Corbetta M. Functional connectivity and neurological recovery. Developmental Psychobiology. 2012;54(3):239-53.

4. Biswal B, Mennes M, Zuo X-N, Gohel S, Kelly C, Smith S, et al. Toward discovery science of human brain function. P Natl Acad Sci USA. 2010;107(10):4734.

5. Sporns O. Structure and function of complex brain networks. Dialogues in clinical neuroscience. 2013;15(3):247-62.

6. Castellanos FX, Di Martino A, Craddock RC, Mehta AD, Milham MP. Clinical applications of the functional connectome. Neuroimage. 2013;80:527.

7. Buckner RL, Vincent JL. Unrest at rest: Default activity and spontaneous network correlations. Neuroimage. 2007;37(4):1091-6.

8. Bressler SL, Menon V. Large-scale brain networks in cognition: emerging methods and principles. Trends in Cognitive Sciences. 2010;14(6):277-90.

9. Bassett SD, Bullmore TE. Human brain networks in health and disease. Current Opinion in Neurology. 2009;22(4):340-7.

10. van Den Heuvel MP, Sporns O. Network hubs in the human brain. Trends in Cognitive Sciences. 2013;17(12):683-96.

11. Bullmore E, Sporns O. The economy of brain network organization. Nature Reviews Neuroscience. 2012;13:336.

12. Crossley N, Fox P, Bullmore E. Meta-connectomics: human brain network and connectivity meta-analyses. Psychological Medicine. 2016;46(5):897-907.

13. Snyder AZ, Raichle ME. A brief history of the resting state: The Washington University perspective. Neuroimage. 2012;62(2):902-10.

14. Sur S, Sinha VK. Event-related potential: An overview. Ind Psychiatry J. 2009;18(1):70-3.

15. Schwartz R, Rozier C, Seidel Malkinson T, Lehongre K, Adam C, Lambrecq V, et al. Comparing stimulus-evoked and spontaneous response of the face-selective multi-units in the human posterior fusiform gyrus. Neurosci Conscious. 2021;2021(2):niab033.

16. Navid MS, Niazi IK, Lelic D, Nedergaard RB, Holt K, Amjad I, et al. Investigating the Effects of Chiropractic Spinal Manipulation on EEG in Stroke Patients. Brain Sci. 2020;10(5).

17. Lelic D, Niazi IK, Holt K, Jochumsen M, Dremstrup K, Yielder P, et al. Manipulation of Dysfunctional Spinal Joints Affects Sensorimotor Integration in the Prefrontal Cortex: A Brain Source Localization Study. Neural Plast. 2016;2016:3704964.

18. Steven Waterstone T, Niazi IK, Navid MS, Amjad I, Shafique M, Holt K, et al. Functional Connectivity Analysis on Resting-State Electroencephalography Signals Following Chiropractic Spinal Manipulation in Stroke Patients. Brain Sci. 2020;10(9).

19. Beissner F, Meissner K, Bar KJ, Napadow V. The Autonomic Brain: An Activation Likelihood Estimation Meta-Analysis for Central Processing of Autonomic Function. J Neurosci. 2013;33(25):10503-+.

20. McCorry LK. Physiology of the autonomic nervous system. Am J Pharm Educ. 2007;71(4):78.

21. Zygmunt A, Stanczyk J. Methods of evaluation of autonomic nervous system function. Arch Med Sci. 2010;6(1):11-8.

22. Miyamoto T, Kawada T, Yanagiya Y, Inagaki M. Cardiac sympathetic nerve stimulation does not attenuate dynamic vagal control of heart rate via alpha-adrenergic mechanism. American Journal of Physiology. 2004;56(2):H860-H5.

23. Hayano J. Introduction to Heart Rate Variability. In: Iwase S, Hayano J, Orimo S, editors. Clinical Assessment of the Autonomic Nervous System. Tokyo: Springer Japan; 2017. p. 109-27.

24. Shaffer F, McCraty R, Zerr CL. A healthy heart is not a metronome: an integrative review of the heart's anatomy and heart rate variability. Frontiers in psychology. 2014;5:1040-.

25. Michael S, Graham KS, Davis GMO. Cardiac Autonomic Responses during Exercise and Post-exercise Recovery Using Heart Rate Variability and Systolic Time Intervals-A Review. Front Physiol. 2017;8:301.

26. Mansouri S, Alhadidi T, Chabchoub S, Salah RB. Impedance cardiography: recent applications and developments. Biomedical Research. 2018;29(19):3542-52.

27. Amin R, Faghih RT. Physiological characterization of electrodermal activity enables scalable near real-time autonomic nervous system activation inference. PLoS Comput Biol. 2022;18(7):e1010275.

28. Northcote RJ, Cooke MB. How useful are the cold pressor test and sustained isometric handgrip exercise with radionuclide ventriculography in the evaluation of patients with coronary artery disease? Br Heart J. 1987;57(4):319-28.

29. Kent C. Heart rate variability to assess the changes in autonomic nervous system function associated with vertebral subluxation. Res Rev Neurosci. 2017;1:14-21.

30. Welch A, Boone R. Sympathetic and parasympathetic responses to specific diversified adjustments to chiropractic vertebral subluxations of the cervical and thoracic spine. J Chiropr Med. 2008;7(3):86-93.

31. Haas AL, Russell D. Sustained improvement of heart rate variability in patients undergoing a program of chiropractic care: A retrospective case series. Chiropractic Journal of Australia (Online). 2017;45(4):338-58.

32. Kovanur Sampath K, Tumilty S, Wooten L, Belcher S, Farrell G, Gisselman AS. Effectiveness of spinal manipulation in influencing the autonomic nervous system - a systematic review and meta-analysis. J Man Manip Ther. 2024;32(1):10-27.

33. Haavik H, Murphy B. The role of spinal manipulation in addressing disordered sensorimotor integration and altered motor control. Journal of Electromyography and Kinesiology. 2012;22(5):768-76.

34. Henderson CN. The basis for spinal manipulation: Chiropractic perspective of indications and theory. J Electromyogr Kinesiol. 2012.

35. Haavik Taylor H, Holt K, Murphy B. Exploring the neuromodulatory effects of the vertebral subluxation and chiropractic care. Chiropractic Journal of Australia. 2010;40(1):37 - 44.

36. Haavik H, Kumari N, Holt K, Niazi IK, Amjad I, Pujari AN, et al. The contemporary model of vertebral column joint dysfunction and impact of high-velocity, low-amplitude controlled vertebral thrusts on neuromuscular function. European Journal of Applied Physiology. 2021;121(10):2675-720.

37. Haavik H, Niazi IK, Kumari N, Amjad I, Duehr J, Holt K. The Potential Mechanisms of High-Velocity, Low-Amplitude, Controlled Vertebral Thrusts on Neuroimmune Function: A Narrative Review. Medicina. 2021;57(6):536.

38. Jobert M, Wilson FJ, Ruigt GSF, Brunovsky M, Prichep LS, Drinkenburg WHIM. Guidelines for the Recording and Evaluation of Pharmaco-EEG Data in Man: The International Pharmaco-EEG Society (IPEG). Neuropsychobiology. 2012;66(4):201-20.

39. Heathers J. Everything Hertz: methodological issues in short-term frequency-domain HRV. Frontiers In Physiology. 2014;5.

40. Laborde S, Mosley E, Thayer JF. Heart Rate Variability and Cardiac Vagal Tone in Psychophysiological Research - Recommendations for Experiment Planning, Data Analysis, and Data Reporting. Frontiers in psychology. 2017;8:213-.

41. Lohmann G, Margulies DS, Horstmann A, Pleger B, Lepsien J, Goldhahn D, et al. Eigenvector Centrality Mapping for Analyzing Connectivity Patterns in fMRI Data of the Human Brain (Eigenvector Centrality Maps). Plos One. 2010;5(4):e10232.

42. Rossi P, Andriesse GI, Oey PL, Wieneke GH, Roelofs JMM, Akkermans LMA. Stomach distension increases efferent muscle sympathetic nerve activity and blood pressure in healthy humans. Journal of the Neurological Sciences. 1998;161(2):148-55.

43. Fagius J, Karhuvaara S. Sympathetic activity and blood pressure increases with bladder distension in humans. Hypertension. 1989;14(5):511-7.

44. Zimmermann-Viehoff F, Thayer J, Koenig J, Herrmann C, Weber CS, Deter H-C. Short-term effects of espresso coffee on heart rate variability and blood pressure in habitual and non-habitual coffee consumers–a randomized crossover study. Nutritional neuroscience. 2016;19(4):169-75.

45. Sondermeijer HP, van Marle AGJ, Kamen P, Krum H. Acute effects of caffeine on heart rate variability. The American Journal of Cardiology. 2002;90(8):906-7.

46. Liao W, Fan Y-S, Yang S, Li J, Duan X, Cui Q, et al. Preservation Effect: Cigarette Smoking Acts on the Dynamic of Influences Among Unifying Neuropsychiatric Triple Networks in Schizophrenia. Schizophrenia bulletin. 2019;45(6):1242.

47. Sjoberg N, Saint DA. A Single 4 mg Dose of Nicotine Decreases Heart Rate Variability in Healthy Nonsmokers: Implications for Smoking Cessation Programs. Nicotine & Tobacco Research. 2011;13(5):369-72.

48. Quintana DS, McGregor IS, Guastella AJ, Malhi GS, Kemp AH. A Meta-Analysis on the Impact of Alcohol Dependence on Short-Term Resting-State Heart Rate Variability: Implications for Cardiovascular Risk. Alcoholism: Clinical and Experimental Research. 2013;37(S1):E23-E9.

49. Quintana DS, Guastella AJ, McGregor IS, Hickie IB, Kemp AH. Moderate alcohol intake is related to increased heart rate variability in young adults: Implications for health and well-being. Psychophysiology. 2013;50(12):1202-8.

50. Sletten DM, Suarez GA, Low PA, Mandrekar J, Singer W. COMPASS 31: a refined and abbreviated Composite Autonomic Symptom Score. Mayo Clin Proc. 2012;87(12):1196-201.

51. Dennis JP, Vander Wal JS. The Cognitive Flexibility Inventory: Instrument Development and Estimates of Reliability and Validity. Cognitive Therapy and Research. 2010;34(3):241-53.

52. Johansson B, Starmark A, Berglund P, Rödholm M, Rönnbäck L. A self-assessment questionnaire for mental fatigue and related symptoms after neurological disorders and injuries. Brain Injury. 2010;24(1):2-12.

53. Lane SJ, Heddle NM, Arnold E, Walker I. A review of randomized controlled trials comparing the effectiveness of hand held computers with paper methods for data collection. BMC Med Inform Decis Mak. 2006;6:23.

54. Dale O, Hagen KB. Despite technical problems personal digital assistants outperform pen and paper when collecting patient diary data. J Clin Epidemiol. 2007;60(1):8-17.

55. Litchfield J, Freeman J, Schou H, Elsley M, Fuller R, Chubb B. Is the future for clinical trials internet-based? A cluster randomized clinical trial. Clin Trials. 2005;2(1):72-9.

56. Corsi-Cabrera M, Galindo-Vilchis L, Del-Río-Portilla Y, Arce C, Ramos-Loyo J. Within-subject reliability and inter-session stability of EEG power and coherent activity in women evaluated monthly over nine months. Clin Neurophysiol. 2007;118(1):9-21.

57. van Diessen E, Numan T, van Dellen E, van Der Kooi AW, Boersma M, Hofman D, et al. Opportunities and methodological challenges in EEG and MEG resting state functional brain network research. Clin Neurophysiol. 2015;126(8):1468-81.

58. Herwig U, Satrapi P, Schönfeldt-Lecuona C. Using the international 10-20 EEG system for positioning of transcranial magnetic stimulation. Brain Topogr. 2003;16(2):95-9.

59. Lewis GF, Furman SA, McCool MF, Porges SW. Statistical strategies to quantify respiratory sinus arrhythmia: are commonly used metrics equivalent? Biol Psychol. 2012;89(2):349-64.

60. Bailey NW, Biabani M, Hill AT, Miljevic A, Rogasch NC, McQueen B, et al. Introducing RELAX: An automated pre-processing pipeline for cleaning EEG data - Part 1: Algorithm and application to oscillations. Clinical Neurophysiology. 2023;149:178-201.

61. Delorme A, Makeig S. EEGLAB: an open source toolbox for analysis of single-trial EEG dynamics including independent component analysis. Journal of neuroscience methods. 2004;134(1):9-21.

62. Oostenveld R, Fries P, Maris E, Schoffelen JM. FieldTrip: Open source software for advanced analysis of MEG, EEG, and invasive electrophysiological data. Comput Intell Neurosci. 2011;2011:156869.

63. Bigdely-Shamlo N, Mullen T, Kothe C, Su K-M, Robbins KA. The PREP pipeline: standardized preprocessing for large-scale EEG analysis. Frontiers in Neuroinformatics. 2015;9.

64. Somers B, Francart T, Bertrand A. A generic EEG artifact removal algorithm based on the multi-channel Wiener filter. Journal of neural engineering. 2018;15(3):036007.

65. Castellanos NP, Makarov VA. Recovering EEG brain signals: Artifact suppression with wavelet enhanced independent component analysis. Journal of neuroscience methods. 2006;158(2):300-12.

66. Pion-Tonachini L, Kreutz-Delgado K, Makeig S. ICLabel: An automated electroencephalographic independent component classifier, dataset, and website. Neuroimage. 2019;198:181-97.

67. Palmer JA, Kreutz-Delgado K, Makeig S. AMICA: An adaptive mixture of independent component analyzers with shared components. Swartz Center for Computatonal Neursoscience, University of California San Diego, Tech Rep. 2012.

68. Delorme A, Palmer J, Onton J, Oostenveld R, Makeig S. Independent EEG Sources Are Dipolar. PLOS ONE. 2012;7(2):e30135.

69. Blechert J, Peyk P, Liedlgruber M, Wilhelm FH. ANSLAB: Integrated multichannel peripheral biosignal processing in psychophysiological science. Behavior Research Methods. 2016;48(4):1528-45.

70. Yugar LBT, Yugar-Toledo JC, Dinamarco N, Sedenho-Prado LG, Moreno BVD, Rubio TA, et al. The Role of Heart Rate Variability (HRV) in Different Hypertensive Syndromes. Diagnostics (Basel). 2023;13(4).

71. Seidman AJ, Bylsma LM, Yang X, Jennings JR, George CJ, Kovacs M. Long-term stability of respiratory sinus arrhythmia among adults with and without a history of depression. Psychophysiology. 2024;61(1):e14427.

72. Cheung MN, Porges SW. Respiratory influences on cardiac responses during attention. Physiological Psychology. 1977;5(1):53-7.

73. Braithwaite JJ, Watson DG, Jones R, Rowe M. A guide for analysing electrodermal activity (EDA) & skin conductance responses (SCRs) for psychological experiments. Psychophysiology. 2013;49(1):1017-34.

74. Lopez-Calderon J, Luck SJ. ERPLAB: an open-source toolbox for the analysis of event-related potentials. Frontiers in Human Neuroscience. 2014;8.

75. Kappenman ES, Farrens JL, Zhang W, Stewart AX, Luck SJ. ERP CORE: An open resource for human event-related potential research. Neuroimage. 2021;225:117465.

76. Beyramienanlou H, Lotfivand N. Shannon's Energy Based Algorithm in ECG Signal Processing. Computational and Mathematical Methods in Medicine. 2017;2017:8081361.

77. Berntson GG, Quigley KS, Jang JF, Boysen ST. An approach to artifact identification: application to heart period data. Psychophysiology. 1990;27(5):586-98.

78. Mellor K, Albury C, Dutton SJ, Eldridge S, Hopewell S. Recommendations for progression criteria during external randomised pilot trial design, conduct, analysis and reporting. Pilot and Feasibility Studies. 2023;9(1):59.

79. Eldridge SM, Chan CL, Campbell MJ, Bond CM, Hopewell S, Thabane L, et al. CONSORT 2010 statement: extension to randomised pilot and feasibility trials. Pilot Feasibility Stud. 2016;2:64.

80. Armstrong LE, Johnson EC. Water Intake, Water Balance, and the Elusive Daily Water Requirement. Nutrients. 2018;10(12).

81. Haque A, Hughes M. Raynaud's phenomenon. Clin Med (Lond). 2020;20(6):580-7.

82. Temprano KK. A Review of Raynaud's Disease. Mo Med. 2016;113(2):123-6.

83. Teresi JA, Yu X, Stewart AL, Hays RD. Guidelines for Designing and Evaluating Feasibility Pilot Studies. Med Care. 2022;60(1):95-103.

84. Khorramdel L, Frebort M. Context Effects on Test Performance. European Journal of Psychological Assessment. 2011;27(2):103-10.

85. Lucas CP. The order effect: reflections on the validity of multiple test presentations. Psychol Med. 1992;22(1):197-202.

86. Silveira L, Ferreira JC, Patino CM. Mixed-effects model: a useful statistical tool for longitudinal and cluster studies. J Bras Pneumol. 2023;49(2):e20230137.

87. Cannard C, Wahbeh H, Delorme A. BrainBeats as an Open-Source EEGLAB Plugin to Jointly Analyze EEG and Cardiovascular Signals. J Vis Exp. 2024(206).